# Linear and nonlinear magneto-optical properties of monolayer MoS$_2$

Chuong V. Nguyen, Nguyen N. Hieu, Do Muoi, Carlos A. Duque, Elmustapha Feddi, Hieu V. Nguyen, Le T. T. Phuong, Bui D. Hoi, and Huynh V. Phuc

# Linear and nonlinear magneto-optical properties of monolayer MoS$_2$

Chuong V. Nguyen,[1,2] Nguyen N. Hieu,[1] Do Muoi,[3] Carlos A. Duque,[4] Elmustapha Feddi,[5] Hieu V. Nguyen,[6] Le T. T. Phuong,[7] Bui D. Hoi,[7] and Huynh V. Phuc[8,a]

[1]*Institute of Research and Development, Duy Tan University, Da Nang 550000, Vietnam*
[2]*Department of Materials Science and Engineering, Le Quy Don Technical University, Hanoi 100000, Vietnam*
[3]*University of Science-VNU.HCM, 227-Nguyen Van Cu Street, District 5, Ho Chi Minh City 700000, Vietnam*
[4]*Grupo de Materia Condensada-UdeA, Instituto de Física, Facultad de Ciencias Exactas y Naturales, Universidad de Antioquia UdeA, Calle 70 No. 52-21, Medellín, Colombia*
[5]*LaMCScI, Group of Optoelectronic of Semiconductors and Nanomaterials, ENSET, Rabat, Mohammed V University in Rabat, Rabat, Morocco*
[6]*Department of Physics, University of Education, The University of Da Nang, Da Nang 550000, Vietnam*
[7]*Center for Theoretical and Computational Physics, University of Education, Hue University, Hue 530000, Vietnam*
[8]*Division of Theoretical Physics, Dong Thap University, Dong Thap 870000, Vietnam*

In this work, using the compact density matrix approach, we study the linear and nonlinear magneto-optical properties of monolayer molybdenum disulfide (MoS$_2$) via an investigation of the absorption coefficients (MOACs) and refractive index changes (RICs). The results are presented as functions of photon energy and external magnetic field. Our results show that the MOACs and the RICs appear as a series of peaks in the inter-band transitions between Landau levels, while the intra-band transitions result in only one peak. Because of the strong spin-orbit coupling, the peaks caused by the spin-up and -down states are different. With the increase in the magnetic field, both MOACs and RICs give a blue-shift and reduce in their amplitudes. These results suggest a potential application of monolayer MoS$_2$ in the optoelectronic technology, magneto-optical, valleytronic, and spintronic devices. *Published by AIP Publishing.* https://doi.org/10.1063/1.5009481

## I. INTRODUCTION

Because of its miraculous electron structure,[1–3] graphene holds some extraordinary transport properties such as the quantum Hall effect,[4–6] dc-conductivity,[7] magneto-optical conductivity,[8–10] phonon-assisted cyclotron resonance,[11–13] and the magneto-optical properties.[14] However, the application of graphene in electronic devices is still limited. The main reason comes from its zero band-gap and extremely weak spin-orbit coupling (SOC).[15–17] From the point of view of these researches, it is necessary to intensively study different materials with a finite band gap, including phosphorene,[18–20] silicene,[21–23] germanene,[24,25] antimonene,[26] stanene,[27–29] and two-dimensional transition-metal dichalcogenides (TMDs) MX$_2$ (with M = Mo, W; X = S, Se).[30–34]

Monolayer molybdenum disulfide (MoS$_2$), a material constituting a hexagonal layer of molybdenum atoms (Mo) sandwiched between two layers of sulfur atoms (S) in a trigonal prismatic structure,[35] is a typical member of the TMD family. Recently, monolayer MoS$_2$ has been demonstrated to be a semiconductor with a strong SOC and a large direct band gap.[32,36–38] Moreover, although having the honeycomb structure of graphene, monolayer MoS$_2$ has massive Dirac fermions,[21,38–40] high thermal stability, and large carrier mobility.[30,41–43] These wonderful properties offer numerous possibilities for monolayer MoS$_2$ as a promising alternative

to graphene in order to become a good candidate for a wide range of applications, including valleytronic and spintronic devices,[39,44–46] photo-luminescence at visible regimes,[47,48] field-effect transistors,[49] and photodetectors with high responsivity.[50]

It is known that magneto-optics are the most important tools to measure experimentally the band structure of metals and semiconductors.[51] That is the reason why the magneto-optical properties have been investigated widely in large numbers of 2D material systems, such as topological insulators,[52,53] WSe$_2$,[54] and Weyl semimetals.[55] Using the Kubo formula, these useful properties have also been reported in silicene,[23,56] in phosphorene,[19,57] and in WSe$_2$ (Ref. 43) monolayers. Though many efforts have been made to investigate the magneto-optical properties of MoS$_2$,[58–61] a detailed investigation of the effect of a magnetic field on the linear and nonlinear optical properties of monolayer MoS$_2$ for both intra-band and inter-band transitions has not received enough attention. Therefore, studying these properties is timely and necessary.

Besides, the linear and nonlinear optical properties of low-dimensional systems have been investigated widely in recent years due to their importance for understanding in detail the response of semiconductors stimulated by an electromagnetic field. While investigating the linear and nonlinear inter-subband optical absorption in symmetric double semi-parabolic quantum wells, Keshavarz and Karimi[62] showed that both the optical incident intensity and the structure parameters really affect the optical characteristics of

a)Electronic mail: hvphuc@dthu.edu.vn

these structures. Ungan *et al.*[63] have theoretically studied the effects of hydrostatic pressure and temperature on the nonlinear optical properties of a parabolic quantum well under an intense laser field. Their results showed that the linear and nonlinear optical properties in a parabolic quantum well under intense laser field can be tuned by changing the hydrostatic pressure and temperature. The linear and nonlinear optical properties have also been investigated in an asymmetric double inverse parabolic quantum well under applied electric and magnetic field,[64] in a spherical dome shell,[65] in a parabolic quantum well with double barriers,[66] in two-dimensional quantum rings,[67] in a quantum disk with flat cylindrical geometry,[68] and in a spherical core/shell quantum dots.[69,70] However, a detailed investigation of the linear and nonlinear optical absorption coefficients (OACs) and refractive index changes (RICs) in monolayer MoS$_2$ in the presence of a quantized magnetic field is still lacking.

In this work, we investigate the linear and nonlinear OACs in a perpendicular magnetic field, recalled molybdenum disulfide (MoS$_2$) via an investigation of the absorption coefficients (MOACs), and RICs in monolayer MoS$_2$. Using the density matrix theory, we evaluate the MOACs and RICs for transitions between the two bands. We consider the MOACs and RICs as functions of the incident photon energy and external magnetic field for both intra-band and inter-band transitions. The paper is organized as follows: In Sec. II, we present the theoretical framework; the numerical results and discussion are provided in Sec. III, and finally, the conclusions are given in Sec. IV.

## II. THEORETICAL FRAMEWORK

We consider monolayer MoS$_2$ in the $(x, y)$ plane. In the presence of a uniform static perpendicular magnetic field $\mathbf{B} = (0, 0, B)$ applied along the $z$-direction, the single-carrier Hamiltonian in the system can be written as follows:[32,60,71]

$$\mathcal{H} = at(\eta k_x \sigma_x + k_y \sigma_y) + (\bar{\Delta} - s\eta\bar{\lambda})\sigma_z + s\eta\bar{\lambda}, \quad (1)$$

where $a = 3.193$ Å and $t = 1.1$ eV are, respectively, the lattice constant and the hopping integral, the valley index $\eta = \pm 1$ refers to the $K$ and $K'$ valleys, $\bar{\Delta} = \Delta/2$, $\bar{\lambda} = \lambda/2$ with $\Delta = 1.66$ eV and $\lambda = 75$ meV being, respectively, the energy gap and SOC strength,[72] $\mathbf{k} = (k_x, k_y)$ is the carrier momentum, $\sigma_x$, $\sigma_y$, and $\sigma_z$ are the Pauli matrices for the two basic functions, and the spin index $s = \pm 1$ stands for spin-up and -down. Note that the defected effects are also important in tuning and modifying various properties of semiconducting materials.[73,74] However, the main purpose of this work is to study the linear and nonlinear magneto-optical properties with the help of the magneto-optical absorption coefficients and refractive index changes of monolayer MoS$_2$ under the applied magnetic field. Therefore, we neglect the defected effects in the present study. The energy spectrum $E_\alpha$ associated with the electronic states $|\alpha\rangle = |n, s, p, \eta\rangle$ is given as follows:

$$E_\alpha = E_{nsp\eta} = s\eta\bar{\lambda} + p\sqrt{\bar{\Delta}_{s,\eta}^2 + n(\hbar\omega_c)^2}, \quad n \geq 1, \quad (2)$$

with $n$ being the Landau level (LL) index, $\bar{\Delta}_{s,\eta} = \bar{\Delta} - s\eta\bar{\lambda}$, the band index $p = \pm 1$ is for the conduction and valence

bands, $\hbar\omega_c = at\sqrt{2}/a_c$ is the cyclotron energy with $a_c = (\hbar/eB)^{1/2}$ being the magnetic length and $e$ the absolute value of the electron charge. For $n = 0$, the eigenvalues are

$$E_{0s\eta} = -\eta(\bar{\Delta} - s\bar{\lambda}) + s\bar{\lambda}. \quad (3)$$

Since $\hbar\omega_c \ll \bar{\Delta}_{s\eta}$ the energy spectrum in Eq. (2) could be expressed in a simpler form[61]

$$E_{nsp\eta} = (1 - p)s\eta\bar{\lambda} + p\bar{\Delta} + np\frac{\hbar^2\omega_c^2}{2\bar{\Delta}_{s\eta}}, \quad (4)$$

which shows that the Landau levels depend linearly on $n$ and the magnetic field $B$.

The eigenfunctions for the $K$ valley ($\eta = +1$) are

$$\Phi_{n,s}^{p,+1}(\mathbf{r}, k_y) = \frac{e^{ik_y y}}{\sqrt{L_{n,s}^{p,+1}}} \begin{pmatrix} \Lambda_{n,s}^{p,+1}\phi_{n-1}(x - x_0) \\ \phi_n(x - x_0) \end{pmatrix}. \quad (5)$$

Here, $\phi_n(x - x_0)$ represents the harmonic oscillator eigenfunction, centered at $x_0 = a_c^2 k_y$, and $L_{n,s}^{p,\eta} = (\Lambda_{n,s}^{p,\eta})^2 + 1$ with $\Lambda_{n,s}^{p,\eta} = \sqrt{n}\hbar\omega_c[(1 - p\eta)\bar{\Delta}_{s\eta} - np\eta\hbar^2\omega_c^2/2\bar{\Delta}_{s\eta}]^{-1}$. The eigenfunctions for the $K'$ valley ($\eta = -1$) are obtained from Eq. (5) by exchanging $\phi_n(x - x_0)$ and $\phi_{n-1}(x - x_0)$.

With the help of Eq. (5), the dipole matrix element, $M_{\alpha'\alpha} = e\langle\alpha'|x|\alpha\rangle$, for $x$-polarized incident radiation, is calculated as follows:

$$M_{\alpha'\alpha} = e(\Lambda_{n+1,s}^{p,\pm 1}\Lambda_{n'+1,s'}^{p',\pm 1} + 1)\Big[x_0\delta_{n',n} + (a_c/\sqrt{2}) \\ \times (\sqrt{n}\delta_{n',n-1} + \sqrt{n+1}\delta_{n',n+1})\Big]\delta_{k_y',k_y}. \quad (6)$$

Hence, using the fact that $M_{\alpha'\alpha'} - M_{\alpha\alpha} = 0$ to the expressions of linear and nonlinear optical absorption coefficients for transitions between the two bands $|\alpha\rangle$ and $|\alpha'\rangle$ of Refs. 62–67, we obtain the total optical absorption coefficients

$$\beta(\Omega, I) = \beta^{(1)}(\Omega) + \beta^{(3)}(\Omega, I), \quad (7)$$

where $\beta^{(1)}(\Omega)$ and $\beta^{(3)}(\Omega, I)$ are the linear and third-order nonlinear terms of the optical absorption coefficients, respectively, given as

$$\beta^{(1)}(\Omega) = \Omega\sqrt{\frac{\mu}{\epsilon_r}}\frac{|M_{\alpha'\alpha}|^2 n_e\hbar\Gamma_0}{(E_{\alpha'\alpha} - \hbar\Omega)^2 + (\hbar\Gamma_0)^2}, \quad (8)$$

$$\beta^{(3)}(\Omega, I) = -2\Omega\sqrt{\frac{\mu}{\epsilon_r}}\left(\frac{I}{\epsilon_0 n_r c}\right)\frac{|M_{\alpha'\alpha}|^4 n_e\hbar\Gamma_0}{\Big[(E_{\alpha'\alpha} - \hbar\Omega)^2 + (\hbar\Gamma_0)^2\Big]^2}, \quad (9)$$

where $\hbar\Omega$ is the incident photon energy, $\mu$ is the magnetic permeability, $\epsilon_r$ is the real part of the permittivity, $n_e$ is the carrier density, $\Gamma_0$ is the non-diagonal matrix element known as relaxation rate, $E_{\alpha'\alpha} = E_{\alpha'} - E_\alpha$ is the energy difference between the two bands, $I$ is the optical intensity of the incident photon which excites the system and leads to the optical transitions, $c$ is the speed of light, $\epsilon_0$ is the permittivity of free space, and $n_r$ is the refractive index.

The total relative index changes with the incident photon energy $\hbar\Omega$ and the system optical radiation intensity $I$ can be expressed as[67,68]

$$\frac{\Delta n(\Omega, I)}{n_r} = \frac{\Delta n^{(1)}(\Omega)}{n_r} + \frac{\Delta n^{(3)}(\Omega, I)}{n_r}, \qquad (10)$$

where the linear and nonlinear relative refractive index changes are

$$\frac{\Delta n^{(1)}(\Omega)}{n_r} = \frac{n_e |M_{\alpha'\alpha}|^2}{2n_r^2 \epsilon_0} \left[ \frac{E_{\alpha'\alpha} - \hbar\Omega}{(E_{\alpha'\alpha} - \hbar\Omega)^2 + (\hbar\Gamma_0)^2} \right], \qquad (11)$$

$$\frac{\Delta n^{(3)}(\Omega, I)}{n_r} = -\frac{\mu c |M_{\alpha'\alpha}|^4}{n_r^3 \epsilon_0} \frac{n_e I (E_{\alpha'\alpha} - \hbar\Omega)}{\left[ (E_{n'n} - \hbar\Omega)^2 + (\hbar\Gamma_0)^2 \right]^2}. \qquad (12)$$

In Sec. III, the analytical expressions above will be used to consider the numerical calculations in more detail.

## III. RESULTS AND DISCUSSION

In this section, we will calculate and analyze the behaviors of the linear and nonlinear MOACs and RICs as functions of the incident photon energy in monolayer MoS$_2$. The parameters used in our calculations are as follows:[14,75,76] $n_r = 4.828$, $I = 5$ MW/m$^2$, and $\hbar\Gamma_0 = 0.1\sqrt{B}$ meV. The 2D carrier density of $2 \times 10^{12}$ cm$^{-2}$ (Ref. 77) and the effective layer thickness of 6.145 Å (Ref. 78) lead to the 3D carrier density $n_e = 3.255 \times 10^{19}$ cm$^{-3}$. Our calculations are for $k_y = 0$, i.e., $x_0 = 0$. It means that according to Eq. (6), the selections rules lead to the fact that only transitions with $n' = n \pm 1$ are allowed. Besides, because of the symmetry of the $K$ and $K'$ valleys,[61] we will only investigate the case of $\eta = \eta' = 1$ and ignore the valley indices $\eta$ and $\eta'$ in the following.

Figure 1 shows the dependence of the linear, the third-order nonlinear, and the total MOACs for intra-band transitions on photon energy at $B = 10$ T. These transitions comply with the selection rules $n' = n \pm 1$, $s = s'$, and $p = p' = 1$, where the absorbed photon energies satisfy the condition
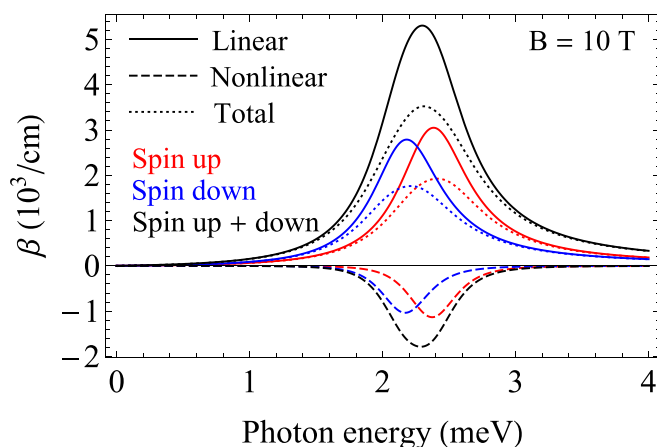
$$\hbar\Omega = (\hbar\omega_c)^2 / (2\bar{\Delta}_{s,1}). \qquad (13)$$

Due to the strong SOC, which has been demonstrated from the transition-metal $d$ orbitals,[71,72] the peaks caused by the spin-up and -down states are different. For instance, at $B = 10$ T, the absorption peaks due to spin-up and -down are located at $\hbar\Omega = 2.362$ meV and $2.158$ meV, respectively. The values of photon frequency at these peaks are in the THz range, likely in graphene[14,79] and some other 2D materials.[52,55,56] For each value of the magnetic field, the distance between the Landau levels is maintained. Therefore, all of the absorption peaks due to intra-band transitions coincide, leading to only one absorption peak, for each value of spin, as observed in Fig. 1. This behavior is in agreement with that in monolayer phosphorene[80] but in dissonance with that in graphene.[14] This can be explained by the fact that, in MoS$_2$ and phosphorene, the Landau levels linearly depend on $n$, whereas in graphene, the Landau levels are proportional to $\sqrt{n}$.

Figure 2 shows the dependence of the linear, the third-order nonlinear, and the total MOACs for conduction intra-band transition on photon energy for three different values of the magnetic field. The MOACs are calculated for the sum of both spins-up and -down cases. Because of the opposite signs between the linear and the third-order nonlinear MOACs, the total MOAC would have been lessened by the contribution of the nonlinear term. It can be seen from the figure that since the enhancement in the cyclotron energy $\hbar\omega_c$ with the increasing magnetic field $B$, MOACs give a blue-shift when the magnetic field increases. Besides, while the linear and third-order nonlinear MOACs decrease, the total one increases with increasing magnetic field. These results can be explained from the magnetic field dependence of the dipole matrix element [see Eq. (6)]: when the magnetic field increases, the dipole matrix element, $M_{\alpha'\alpha}$, lessens due to the diminishing in the magnetic length, $a_c$, resulting in a drop in the linear and third-order nonlinear MOACs. Moreover, we can see from Eqs. (8) and (9) that since the linear part of the coefficient is proportional to $|M_{\alpha'\alpha}|^2$ while the nonlinear one depends on $|M_{\alpha'\alpha}|^4$, the latter decreases



FIG. 1. The linear, the third-order nonlinear, and the total MOACs for intra-band transitions as a function of photon energy at $B = 10$ T.
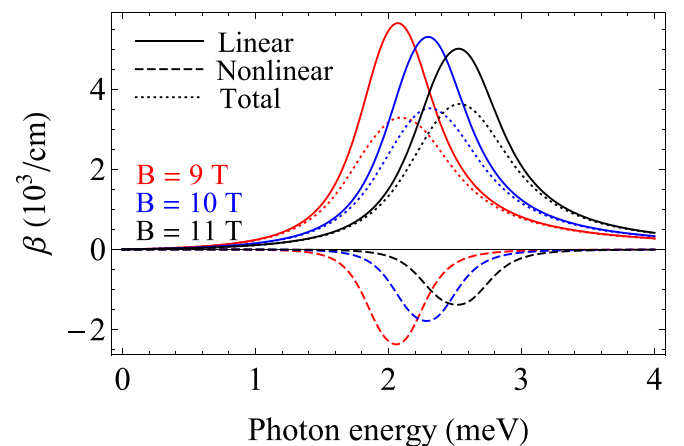


FIG. 2. The linear, the third-order nonlinear, and the total MOACs for intra-band transitions as functions of photon energy for three different values of magnetic field.
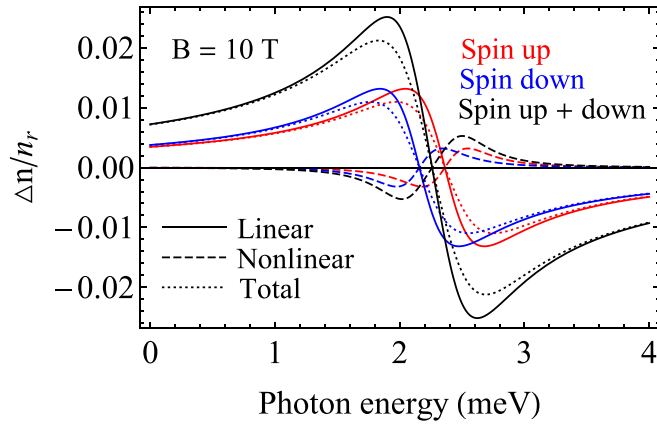
FIG. 3. The linear, the third-order nonlinear, and the total RICs for intra-band transition as functions of photon energy at $B = 10\,\text{T}$.
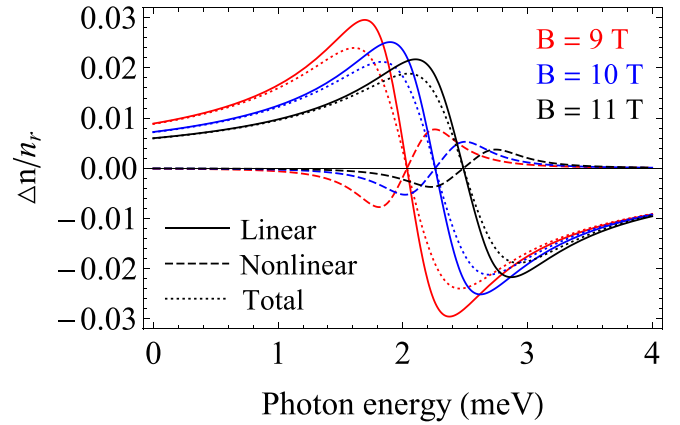


FIG. 4. The linear, the third-order nonlinear, and the total RICs for intra-band transition as functions of photon energy for three different values of the magnetic field.

faster with an increasing magnetic field than the former does. This leads to an increase in the total MOAC with an increasing magnetic field as shown in Fig. 2. These results are in good agreement with previous works.[14,64,68,80]

In Fig. 3 the linear, the third-order nonlinear, and the total relative refractive index changes for intra-band transition are shown as functions of photon energy. The results are calculated for both the spins-up and -down cases. Similar to the case of the absorption coefficients, the transition energies due to spin-up are little bigger than those due to spin-down, resulting in slightly larger absorbed photon energies in the case of spin-up. Note that the absorbed photon energies are inversely proportional to $\bar{\Delta}_{s,1} = \bar{\Delta} - s\bar{\lambda}$ [see Eq. (13)]. It is clear that the quantity $\bar{\Delta}_{1,1} = \bar{\Delta} - \bar{\lambda}$ ($s = 1$, spin-up) is smaller than $\bar{\Delta}_{-1,1} = \bar{\Delta} + \bar{\lambda}$ ($s = -1$, spin-down). This explains the blue-shift behavior of the spin-up in comparison with the spin-down case.

Figure 4 shows the dependence of the linear, the third-order nonlinear and the total RICs for the intra-band transition on the photon energy for different values of the magnetic field. The results are calculated as the sum of both spins -up and -down. From the figure, we can see that when the magnetic field increases, the RICs give a blue-shift and reduce in magnitude. The blue-shift behavior is explained by the enhancement of the transition energies, while the drop in magnitude comes from the reduction of the dipole matrix element when the magnetic field increases.

Having discussed the magneto-optical properties for the intra-band transitions, we now turn our attention to the investigation of the inter-band transitions. In Fig. 5, we depict the dependence of MOACs for the inter-band transitions on photon energy at $B = 10\,\text{T}$ for both spin-up and -down states. It is clear that the strong SOC is the cause of the Landau levels splitting in $MoS_2$ leading to the segregation of transition energies for the spin-up and -down states, as shown in Figs. 5(a) and 5(b). This is completely different from that in graphene,[14,81] phosphorene,[80] and some other 2D systems,[52,56] but agrees with previous work performed for monolayer $MoS_2$ where the electron–phonon interaction is taken into account.[61] Besides, the large band-gap in $MoS_2$ leads to the observation at the visible frequency range of the inter-band transition energies. This is in good agreement with previous works.[38,61] Besides, in comparison with the intra-band transitions, we can see here that: (i) the inter-band transitions are present in a series of peaks corresponding to the transitions from the occupied valence bands to the bare conduction bands; (ii) these inter-band transition peaks appear in the visible regime, which results from the large band-gap of monolayer $MoS_2$. Moreover, in contrast to the results reported in previous works calculated for monolayer phosphorene[19,80] and monolayer $WSe_2$,[43] here, the amplitude of the inter-band transition peaks is much higher than that of the intra-band transitions. We hope that this conflict will be solved in the
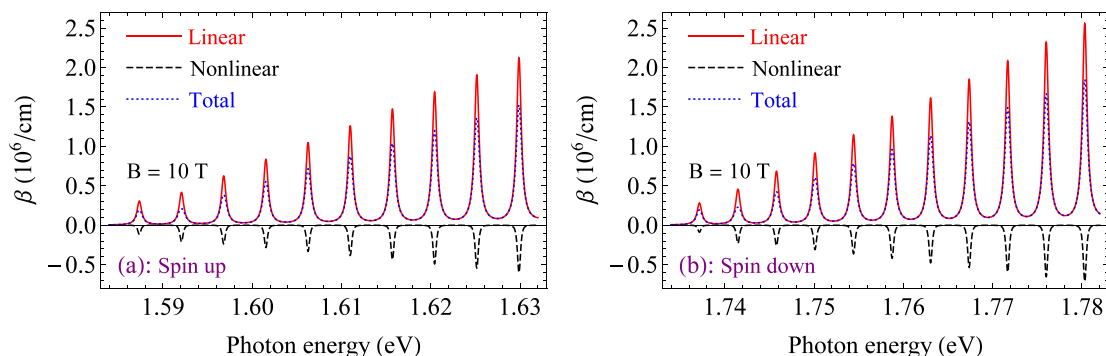


FIG. 5. The linear, the third-order nonlinear, and the total MOACs for inter-band transitions as functions of photon energy at $B = 10\,\text{T}$. The left (a) and right (b) panels correspond to the spin-up and -down cases and differ only in the photon energy range (x-axis).
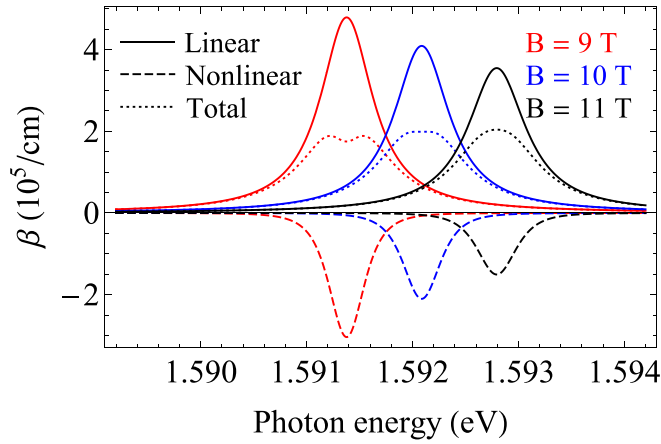
FIG. 6. The linear, the third-order nonlinear, and the total MOACs for the individual inter-band $n = 1 \rightarrow n' = 2$ transition as functions of photon energy for different values of magnetic field. The result is calculated for the spin-up case.



FIG. 8. The linear, the third-order nonlinear, and the total RICs for the inter-band $n = 1 \rightarrow n' = 2$ transitions as functions of photon energy for different values of magnetic field. The result is calculated for the spin-up case.

near future when we will have accurate experimental observation.

The effects of the magnetic field on the absorption coefficients are presented in Fig. 6, where we show the dependence of the linear, the third-order nonlinear, and the total MOACs for a specific transition on photon energy for three different values of the magnetic field. Since the optical transitions due to spin-up and spin-down are similar, we only show the spin-up case here, but the results could be also validated for the other case. Similar to the intra-band transitions (see Fig. 2), the reduction in the MOACs with an increase in the magnetic field is continuously held for the inter-band transitions. The physical explanation can be obtained from the increase in the transition energies when the magnetic field increases.

In Fig. 7, we depict the dependence of the linear, the third-order nonlinear, and the total relative refractive index changes for the inter-band transitions on photon energy at $B = 10$ T. Similar to the absorption coefficients, the RICs also appear here in a series of peaks, but the magnitude of the RICs for the inter-band transitions are much smaller than those for the intra-band transitions. Besides, the magnitudes of the RICs increase with the Landau level index. This result is in good agreement with the one reported in previous works for phosphorene[80] and graphene[14] and could be explained qualitatively as follows: From Eqs. (11) and (12), we can see

that the amplitudes of the RICs increase with the Landau level index through the dipole matrix element $M_{\alpha'\alpha}$. Therefore, the magnitude of the RICs is higher with increasing Landau level index.

Finally, the dependence of the linear, third-order nonlinear, and total RICs for the individual inter-band $n = 1 \rightarrow n' = 2$ transition on photon energy for different values of the magnetic field is shown in Fig. 8. Through the absorption of a photon, the RICs due to inter-band transition shift toward higher photon energies and reduce in magnitude when the magnetic field increases. These results are similar to those for the intra-band transitions described in Fig. 4. However, unlike in phosphorene[80] and in graphene,[14] here we can see that, in monolayer MoS$_2$, the third-order nonlinear term gives a significant contribution to the total RIC. This may come from the fact that the dipole matrix element in monolayer MoS$_2$ is stronger than that in phosphorene and graphene.

## IV. CONCLUSIONS

In this work, using the compact density matrix approach, we have investigated the linear, the third-order nonlinear, and the total magneto-optical responses in monolayer MoS$_2$. All possible optical transitions satisfy the selection rules $n' = n \pm 1$, and $s = s'$ with the absorbed photon energies defined as $\hbar\Omega = (\hbar\omega_c)^2/(2\bar{\Delta}_{s,1})$. For the inter-band optical transitions $(p \neq p')$, the absorption spectrum consists of a
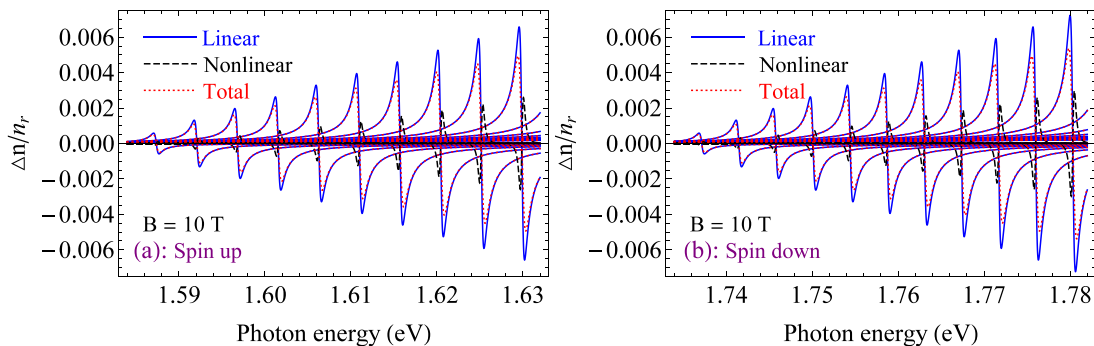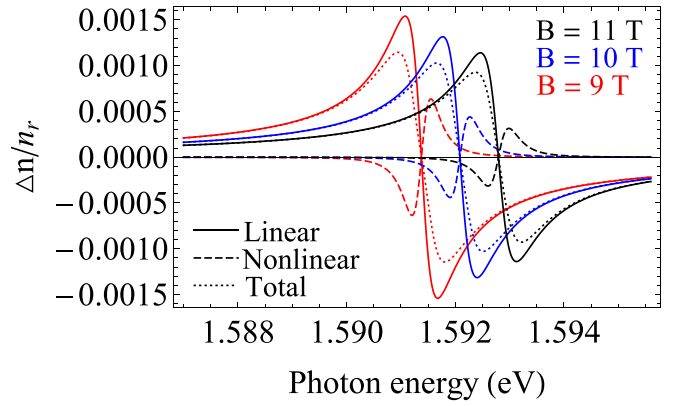


FIG. 7. The linear, the third-order nonlinear, and the total RICs for inter-band transitions as functions of photon energy at $B = 10$ T. The left (a) and right (b) panels correspond to the spin-up and -down cases and differ only in the photon energy range (x-axis).

series of peaks which are located in the visible range. Meanwhile, for the intra-band optical transitions ($p = p' = 1$), these spectra appear in only one peak and are located in the microwave to THz range. Because of the strong SOC, the absorption peaks caused by the spin-up and -down states are different. Besides, the MOACs and RICs are strongly affected by the magnetic field. When the magnetic field increases, the MOACs and RICs shift toward higher energies and reduce in magnitude. We hope that these results would be significant in potential applications of optoelectronic, magneto-optical, valleytronic, and spintronic devices.

## ACKNOWLEDGMENTS

[1] K. S. Novoselov, A. K. Geim, S. V. Morozov, D. Jiang, Y. Zhang, S. V. Dubonos, I. V. Grigorieva, and A. A. Firsov, Science **306**, 666 (2004).

[2] K. S. Novoselov, D. Jiang, F. Schedin, T. J. Booth, V. V. Khotkevich, S. V. Morozov, and A. K. Geim, Proc. Natl. Acad. Sci. U.S.A. **102**, 10451 (2005).

[3] N. M. R. Peres, Rev. Mod. Phys. **82**, 2673 (2010).

[4] Z. Jiang, Y. Zhang, Y.-W. Tan, H. Stormer, and P. Kim, Solid State Commun. **143**, 14 (2007).

[5] V. P. Gusynin and S. G. Sharapov, Phys. Rev. Lett. **95**, 146801 (2005).

[6] X. Wu, Y. Hu, M. Ruan, N. K. Madiomanana, J. Hankinson, M. Sprinkle, C. Berger, and W. A. de Heer, Appl. Phys. Lett. **95**, 223108 (2009).

[7] K. Nomura and A. H. MacDonald, Phys. Rev. Lett. **98**, 076602 (2007).

[8] V. P. Gusynin, S. G. Sharapov, and J. P. Carbotte, J. Phys.: Condens. Matter **19**, 026222 (2007).

[9] C. H. Yang, F. M. Peeters, and W. Xu, Phys. Rev. B **82**, 205428 (2010).

[10] J.-M. Poumirol, P. Q. Liu, T. M. Slipchenko, A. Y. Nikitin, L. Martin-Moreno, J. Faist, and A. B. Kuzmenko, Nat. Commun. **8**, 14626 (2017).

[11] H. V. Phuc and N. N. Hieu, Opt. Commun. **344**, 12 (2015).

[12] H. V. Phuc and L. Dinh, Mater. Chem. Phys. **163**, 116 (2015).

[13] H. V. Phuc, Superlattices Microstruct. **88**, 518 (2015).

[14] C. V. Nguyen, N. N. Hieu, C. A. Duque, N. A. Poklonski, V. V. Ilyasov, N. V. Hieu, L. Dinh, Q. K. Quang, L. V. Tung, and H. V. Phuc, Opt. Mater. **69**, 328 (2017).

[15] B. Dlubak, M.-B. Martin, C. Deranlot, B. Servet, S. Xavier, R. Mattana, M. Sprinkle, C. Berger, W. A. De Heer, F. Petroff, A. Anane, P. Seneor, and A. Fert, Nat. Phys. **8**, 557 (2012).

[16] L. Brey, Phys. Rev. B **92**, 235444 (2015).

[17] X. Zhang and G. Lu, Carbon **108**, 215 (2016).

[18] A. N. Rudenko and M. I. Katsnelson, Phys. Rev. B **89**, 201408 (2014).

[19] M. Tahir, P. Vasilopoulos, and F. M. Peeters, Phys. Rev. B **92**, 045420 (2015).

[20] Y. Jiang, R. Roldán, F. Guinea, and T. Low, Phys. Rev. B **92**, 085408 (2015).

[21] P. Vogt, P. De Padova, C. Quaresima, J. Avila, E. Frantzeskakis, M. C. Asensio, A. Resta, B. Ealet, and G. Le Lay, Phys. Rev. Lett. **108**, 155501 (2012).

[22] L. Chen, C.-C. Liu, B. Feng, X. He, P. Cheng, Z. Ding, S. Meng, Y. Yao, and K. Wu, Phys. Rev. Lett. **109**, 056804 (2012).

[23] C. J. Tabert and E. J. Nicol, Phys. Rev. B **88**, 085434 (2013).

[24] X. Chen, Q. Yang, R. Meng, J. Jiang, Q. Liang, C. Tan, and X. Sun, J. Mater. Chem. C **4**, 5434 (2016).

[25] P. Liang, Y. Liu, S. Xing, H. Shu, and B. Tai, Solid State Commun. **226**, 19 (2016).

[26] J. Ji, X. Song, J. Liu, Z. Yan, C. Huo, S. Zhang, M. Su, L. Liao, W. Wang, Z. Ni, Y. Hao, and H. Zeng, Nat. Commun. **7**, 13352 (2016).

[27] Y. Xu, B. Yan, H.-J. Zhang, J. Wang, G. Xu, P. Tang, W. Duan, and S.-C. Zhang, Phys. Rev. Lett. **111**, 136804 (2013).

[28] M. Wang, L. Liu, C.-C. Liu, and Y. Yao, Phys. Rev. B **93**, 155412 (2016).

[29] B. Peng, H. Zhang, H. Shao, Y. Xu, X. Zhang, and H. Zhu, Sci. Rep. **6**, 20225 (2016).

[30] B. Radisavljevic, A. Radenovic, J. Brivio, V. Giacometti, and A. Kis, Nat. Nanotechnol. **6**, 147 (2011).

[31] M. S. Fuhrer and J. Hone, Nat. Nanotechnol. **8**, 146 (2013).

[32] D. Xiao, G.-B. Liu, W. Feng, X. Xu, and W. Yao, Phys. Rev. Lett. **108**, 196802 (2012).

[33] H.-Z. Lu, W. Yao, D. Xiao, and S.-Q. Shen, Phys. Rev. Lett. **110**, 016806 (2013).

[34] X. Li, F. Zhang, and Q. Niu, Phys. Rev. Lett. **110**, 066803 (2013).

[35] K. F. Mak, K. He, J. Shan, and T. F. Heinz, Nat. Nanotechnol. **7**, 494 (2012).

[36] A. Scholz, T. Stauber, and J. Schliemann, Phys. Rev. B **88**, 035135 (2013).

[37] P. M. Krstajić, P. Vasilopoulos, and M. Tahir, Phys. Rev. B **94**, 085413 (2016).

[38] M. Tahir, P. Vasilopoulos, and F. M. Peeters, Phys. Rev. B **93**, 035406 (2016).

[39] T. Cao, G. Wang, W. Han, H. Ye, C. Zhu, J. Shi, Q. Niu, P. Tan, E. Wang, B. Liu, and J. Feng, Nat. Commun. **3**, 887 (2012).

[40] M. Tahir, A. Manchon, and U. Schwingenschlögl, Phys. Rev. B **90**, 125438 (2014).

[41] H. Fang, S. Chuang, T. C. Chang, K. Takei, T. Takahashi, and A. Javey, Nano Lett. **12**, 3788 (2012).

[42] H. Wang, L. Yu, Y.-H. Lee, Y. Shi, A. Hsu, M. L. Chin, L.-J. Li, M. Dubey, J. Kong, and T. Palacios, Nano Lett. **12**, 4674 (2012).

[43] M. Tahir and P. Vasilopoulos, Phys. Rev. B **94**, 045415 (2016).

[44] H. Zeng, J. Dai, W. Yao, D. Xiao, and X. Cui, Nat. Nanotechnol. **7**, 490 (2012).

[45] Y. J. Zhang, T. Oka, R. Suzuki, J. T. Ye, and Y. Iwasa, Science **344**, 725 (2014).

[46] K. F. Mak, K. L. McGill, J. Park, and P. L. McEuen, Science **344**, 1489 (2014).

[47] A. Splendiani, L. Sun, Y. Zhang, T. Li, J. Kim, C.-Y. Chim, G. Galli, and F. Wang, Nano Lett. **10**, 1271 (2010).

[48] Q. H. Wang, K. Kalantar-Zadeh, A. Kis, J. N. Coleman, and M. S. Strano, Nat. Nanotechnol. **7**, 699 (2012).

[49] D. Wu, X. Li, L. Luan, X. Wu, W. Li, M. N. Yogeesh, R. Ghosh, Z. Chu, D. Akinwande, Q. Niu, and K. Lai, Proc. Natl. Acad. Sci. U.S.A. **113**, 8583 (2016).

[50] H. S. Lee, S.-W. Min, Y.-G. Chang, M. K. Park, T. Nam, H. Kim, J. H. Kim, S. Ryu, and S. Im, Nano Lett. **12**, 3695 (2012).

[51] X. Zhou, W.-K. Lou, F. Zhai, and K. Chang, Phys. Rev. B **92**, 165405 (2015).

[52] Z. Li and J. P. Carbotte, Phys. Rev. B **88**, 045414 (2013).

[53] M. Lasia and L. Brey, Phys. Rev. B **90**, 075417 (2014).

[54] B. Fallahazad, H. C. P. Movva, K. Kim, S. Larentis, T. Taniguchi, K. Watanabe, S. K. Banerjee, and E. Tutuc, Phys. Rev. Lett. **116**, 086601 (2016).

[55] P. E. C. Ashby and J. P. Carbotte, Phys. Rev. B **87**, 245131 (2013).

[56] C. J. Tabert and E. J. Nicol, Phys. Rev. Lett. **110**, 197402 (2013).

[57] X. Y. Zhou, R. Zhang, J. P. Sun, Y. L. Zou, D. Zhang, W. K. Lou, F. Cheng, G. H. Zhou, F. Zhai, and K. Chang, Sci. Rep. **5**, 12295 (2015).

[58] F. Rose, M. O. Goerbig, and F. Piéchon, Phys. Rev. B **88**, 125438 (2013).

[59] R.-L. Chu, X. Li, S. Wu, Q. Niu, W. Yao, X. Xu, and C. Zhang, Phys. Rev. B **90**, 045427 (2014).

[60] C. M. Wang and X. L. Lei, Phys. Rev. B **92**, 125303 (2015).

[61] C. V. Nguyen, N. N. Hieu, N. A. Poklonski, V. V. Ilyasov, L. Dinh, T. C. Phong, L. V. Tung, and H. V. Phuc, Phys. Rev. B **96**, 125411 (2017).

[62] A. Keshavarz and M. Karimi, Phys. Lett. A **374**, 2675 (2010).

[63] F. Ungan, U. Yesilgul, S. Sakiroglu, M. E. Mora-Ramos, C. A. Duque, E. Kasapoglu, H. Sari, and I. Sökmen, Opt. Commun. **309**, 158 (2013).

[64] E. Al, F. Ungan, U. Yesilgul, E. Kasapoglu, H. Sari, and I. Sökmen, Opt. Mater. **47**, 1 (2015).

[65] K. Guo, G. Liu, L. Huang, and X. Zheng, Opt. Mater. **46**, 361 (2015).

[66] J. Gong, X. X. Liang, and S. L. Ban, J. Appl. Phys. **100**, 023707 (2006).

[67] C. M. Duque, A. L. Morales, M. E. Mora-Ramos, and C. A. Duque, J. Lumin. **143**, 81 (2013).

[68] M. Gambhir, M. Kumar, P. Jha, and M. Mohan, J. Lumin. **143**, 361 (2013).

[69]M. El Haouari, A. Talbi, E. Feddi, H. El Ghazi, A. Oukerroum, and F. Dujardin, Opt. Commun. **383**, 231 (2017).

[70]E. Feddi, A. Talbi, M. Mora-Ramos, M. El Haouari, F. Dujardin, and C. Duque, Physica B **524**, 64 (2017).

[71]W.-Y. Shan, H.-Z. Lu, and D. Xiao, Phys. Rev. B **88**, 125301 (2013).

[72]Z. Y. Zhu, Y. C. Cheng, and U. Schwingenschlögl, Phys. Rev. B **84**, 153402 (2011).

[73]S. Yuan, R. Roldán, M. I. Katsnelson, and F. Guinea, Phys. Rev. B **90**, 041402 (2014).

[74]M. Pandey, F. A. Rasmussen, K. Kuhar, T. Olsen, K. W. Jacobsen, and K. S. Thygesen, Nano Lett. **16**, 2234 (2016).

[75]X. Cui, G.-H. Lee, Y. D. Kim, G. Arefe, P. Y. Huang, C.-H. Lee, D. A. Chenet, X. Zhang, L. Wang, F. Ye, F. Pizzocchero, B. S. Jessen, K.

Watanabe, T. Taniguchi, D. A. Muller, T. Low, P. Kim, and J. Hone, Nat. Nanotechnol. **10**, 534 (2015).

[76]H. Zhang, Y. Ma, Y. Wan, X. Rong, Z. Xie, W. Wang, and L. Dai, Sci. Rep. **5**, 8440 (2015).

[77]K. Kaasbjerg, K. S. Thygesen, and K. W. Jacobsen, Phys. Rev. B **85**, 115317 (2012).

[78]T. Li, Phys. Rev. B **85**, 235407 (2012).

[79]T. Morimoto, Y. Hatsugai, and H. Aoki, Phys. Rev. Lett. **103**, 116803 (2009).

[80]C. V. Nguyen, N. N. Hieu, C. A. Duque, D. Q. Khoa, N. V. Hieu, L. V. Tung, and H. V. Phuc, J. Appl. Phys. **121**, 045107 (2017).

[81]V. Gusynin, S. Sharapov, and J. Carbotte, Phys. Rev. Lett. **98**, 157402 (2007).